

# The influence of acid–base and oxidation–reduction properties of nickel oxysalts on catalytic oxidation of propene

Wincenty Turek · Joanna Strzezik ·  
Agnieszka Krowiak

Received: 1 December 2011 / Accepted: 11 May 2012 / Published online: 26 May 2012  
© Akadémiai Kiadó, Budapest, Hungary 2012

**Abstract** The catalytic activity of nickel oxysalts  $\text{NiCo}_2\text{O}_4$ ,  $\text{NiFe}_2\text{O}_4$ ,  $\text{NiTiO}_3$ ,  $\text{NiMoO}_4$ ,  $\text{Ni}_3(\text{PO}_4)_2$ , with different ionic character of the oxygen bond in the anionic ligand was investigated. The acid–base and redox properties of selected catalysts were studied on the basis of kinetics of isopropyl alcohol conversion. The kinetics of propene oxidation over the catalysts and the activation energy and selectivity of oxidation reactions were determined. Activities of the catalysts in the propene oxidation reaction were compared with their oxidation–reduction and acid–base properties. The influence of the amount and form of chemisorbed oxygen on the propene oxidation pathway was investigated. Over the most active catalysts, the non-destructive propene oxidation towards acrolein is the least selective. Oxysalt catalysts active in oxidation reactions exhibit strong redox properties but direct the process towards destructive oxidation products.

**Keywords** Propene oxidation · Oxygen adsorption · Nickel oxysalts · Oxidation–reduction properties · Acid–base properties

## Introduction

Selective oxidation of lower alkenes receive much attention in fundamental and applied research projects due to the importance of the reaction products for various

---

W. Turek · J. Strzezik (✉) · A. Krowiak  
Institute of Physical Chemistry and Technology of Polymers,  
Silesian University of Technology, Strzody 9, 44-100 Gliwice, Poland  
e-mail: joanna.strzezik@polsl.pl

W. Turek  
e-mail: wincenty.turek@polsl.pl

A. Krowiak  
e-mail: agnieszka.krowiak@polsl.pl

industrial applications [1–3]. More than one-third of worldwide chemical products are produced in catalytic processes using oxide catalysts. Among them, catalysts for selective oxidation are typical examples of heterogeneous metal oxide-type materials, which are used in about 25 % of the worldwide production of organic chemicals [4, 5].

During the oxidation of hydrocarbons over oxide catalysts, two different transition complexes initiate two distinct reaction pathways. When oxygen is activated as ionic species  $O_2^-$  or  $O^-$  in the oxidation process of simple molecules such as  $H_2$ , CO or  $CH_4$ , these forms of oxygen are the main reagents of the full oxidation [6]. Such ionic forms of oxygen can be considered as electrophilic species, which attack olefin molecules in the region of the highest electron density. This kind of electrophilic addition of  $O_2^-$  or  $O^-$  results in the formation of peroxy- or epoxy-complexes, which are only transient products of the degradation of the carbon chain and the total oxidation under the conditions of catalytic oxidation. These reactions can be classified as electrophilic oxidation [7, 8].

The second pathway of heterogeneous oxidation begins with the activation of the hydrocarbon molecule by the abstraction of hydrogen from a carbon atom, which can easily undergo a nucleophilic addition of the  $O_2^-$  ion. It should be emphasised that the  $O_2^-$  ion does not have oxidative properties but is nucleophilic [9]. Subsequent steps of hydrogen abstraction and oxygen addition can be repeated, which leads to selective formation of molecules containing more oxygen atoms. These reactions are classified as nucleophilic oxidation [10].

In this paper, it is shown that the reaction pathway of heterogeneous catalytic oxidation of hydrocarbons over oxysalts depends on the form of chemisorbed oxygen, whereas the forms of chemisorbed oxygen are determined by acid–base and redox properties of the catalyst surface.

In the present study, the catalytic activity of nickel oxysalts ( $NiCo_2O_4$ ,  $NiFe_2O_4$ ,  $NiTiO_3$ ,  $NiMoO_4$ ,  $Ni_3(PO_4)_2$ ) with different ionic character of the oxygen bond in the anionic ligand was investigated. The determination of acid–base and redox properties of selected catalysts was based on measurements of isopropyl alcohol conversion. The activation energies and selectivities of parallel dehydration and dehydrogenation reactions were obtained. The results were correlated with the data concerning the polarity of the bond between the central atom and oxygen in the anions. Catalytic properties of oxysalts were compared with their oxygen sorption capacities, which depend on the electron donor properties of the oxysalt cation (the centre of oxygen adsorption). The activities of the catalysts in the propene oxidation reaction were correlated with their oxidation–reduction and acid–base properties.

## Experimentals and methods

### Preparation of catalysts

Catalysts  $NiCo_2O_4$  and  $NiFe_2O_4$  were prepared using the precipitation method. The first step consisted of metal hydroxide formation by precipitation from the solution of stoichiometric amounts of appropriate metal nitrates (nickel and cobalt or nickel

and iron) using 25 % aqueous ammonia. The second step was the evaporation of water and drying of obtained residue. After that, calcination of samples was performed (6 h). The calcination temperature for  $\text{NiCo}_2\text{O}_4$  was 723 K and for  $\text{NiFe}_2\text{O}_4$  873 K.

$\text{NiTiO}_3$  was obtained by sintering the stoichiometric mixture of titanium dioxide and nickel carbonate at temperature 1623 K for 10 h.

$\text{NiMoO}_4$  was synthesized by precipitation from an aqueous solution of nickel nitrate using ammonium paramolybdate as precipitation agent. The pH of reaction solution was 6.5. The obtained residue was dried and calcined at 873 K for 6 h.

$\text{Ni}_3(\text{PO}_4)_2$  was synthesized by precipitation from an aqueous solution of nickel nitrate, using ammonium phosphate as precipitation agent, at temperature 343 K. The obtained residue was dried and calcined at 733 K for 6 h.

### Catalyst characterization

The XRD analysis of obtained samples was performed using powder diffractometer type Siemens D5005 (AXS-Bruker) in Bragg-Bretano geometry (scan  $\Theta$ – $\Theta$ ). The measurement conditions:  $\text{CuK}_\alpha$  radiation, wavelength  $\lambda = 1.54184 \text{ \AA}$ , graphite monochromator, lamp operating voltage  $U = 55 \text{ kV}$ , intensity of cathode current  $I = 30 \text{ mA}$ , scan range  $10^\circ$ – $90^\circ(2\Theta)$ , step  $0.01^\circ/\text{s}$ .

The specific surface area of all catalysts was established by the BET method using nitrogen adsorption. The measurements were performed under atmospheric pressure at temperature 77.4 K. The apparatus type was Carlo Erba SORPTY 1750.

The XPS analysis was carried out using the equipment VG-ESCA 3Mk II.  $\text{MgK}_\alpha$  monochromatic radiation was applied. The spectra were calibrated on the basis of Au  $4f_{7/2}$  line (84.0 eV) [11]. The examined samples were powdered and placed on gold by surface sedimentation. The charging effect was observed till 2 eV, and calibration was performed using carbon line C 1s (2850 eV).

### Examination of oxygen sorption capacity

Oxygen adsorption was measured using a standard volumetric apparatus. The isotherms of oxygen adsorption (at 653 K) were determined in the range of equilibrium pressures from 0.1 to 25 Pa. Before measurement, samples were heated under vacuum of approximately  $1 \times 10^{-2} \text{ Pa}$  for 16 h at 673 K.

## Kinetic studies

### Isopropyl alcohol conversion

Kinetic measurements were performed in a glass reactor with the inside diameter of 18 mm. The reaction substrate—*isopropyl alcohol* (99.7 % POCH) was diluted with nitrogen. During the measurements, the mole fraction of *isopropyl alcohol* was 0.0179. The flow rate in the catalytic reactor was equal to  $20 \text{ dm}^3 \text{ h}^{-1}$ . Measurements were carried out in the conversion range below 25 %. Approximately

1–2 g of the catalyst was used in each catalytic test (depending on the activity of the catalyst). Before the reaction, all catalysts were conditioned in the reactor at 400 K for 1 h in the nitrogen flow. The products were analyzed using the gas chromatograph with a flame-ionization detector (FID). The organic species were separated on a steel column with a diameter of 3 mm and length of 3 m, filled with 4 % Carbowax 20M on Chromosorb G, AW, DMCS, 80/100 mesh.

### Propene oxidation

The catalytic activity measurements of oxysalts in propene oxidation were performed in gradientless circulation-flow apparatus. The reaction was carried out in a glass reactor with the fixed bed of catalyst. The reaction mixture consisted of oxygen and propene in a mole ratio equal to 2.0. The reaction substrate—propene (POCH) was preliminarily diluted with nitrogen. During the measurements, the mole fraction of propene was 0.0200. The flow rate in the catalytic reactor was equal to  $15 \text{ dm}^3 \text{ h}^{-1}$ . Measurements were carried out in the conversion range below 20 %. Approximately 3–5 g of the catalyst was used in each catalytic test (depending on the activity of the catalyst). Before the reaction, all catalysts were conditioned in the reactor at 573 K for 2 h in the air flow. The products were analyzed using the gas chromatograph. The organic species were separated on a steel column with a diameter of 3 mm and length of 3 m, filled with 4 % Carbowax 20M on Chromosorb G, AW, DMCS, 80/100 mesh, and analyzed with a FID. CO and CO<sub>2</sub> were separated on a steel column with a diameter of 3 mm and length of 2 m, filled with active carbon 60/80 mesh, and analyzed using a thermal conductivity detector (TCD).

## Results and discussion

The properties of nickel oxysalts

The purity and identification of crystalline phases of obtained samples were established on the basis of XRD analysis, whereas the specific surface areas were measured with the BET method. The data of performed analyses are collected in Table 1.

**Table 1** Purity and phase content (XRD) and specific surface area values (BET) of synthesized catalysts

Catalyst	$S_{\text{BET}}$ (m <sup>2</sup> /g)	Structure name	Phase purity
NiCo <sub>2</sub> O <sub>4</sub>	2.5	Spinel	Pure
NiFe <sub>2</sub> O <sub>4</sub>	7.7	Spinel	ca. 3 % Fe <sub>2</sub> O <sub>3</sub> (hematite)
NiTiO <sub>3</sub>	2.6	Perovskite	ca. 5 % TiO <sub>2</sub> (rutile)
NiMoO <sub>4</sub>	11.6	$\alpha$ -NiMoO <sub>4</sub>	ca. 3 % MoO <sub>3</sub> (molybdate)
Ni <sub>3</sub> (PO <sub>4</sub> ) <sub>2</sub>	11.0	Amorphous sample	–

Among all catalysts, only  $\text{Ni}_3(\text{PO}_4)_2$  is amorphous. This amorphous character of nickel phosphate may be due to the very strong glass-forming properties of component  $\text{P}_2\text{O}_5$ .

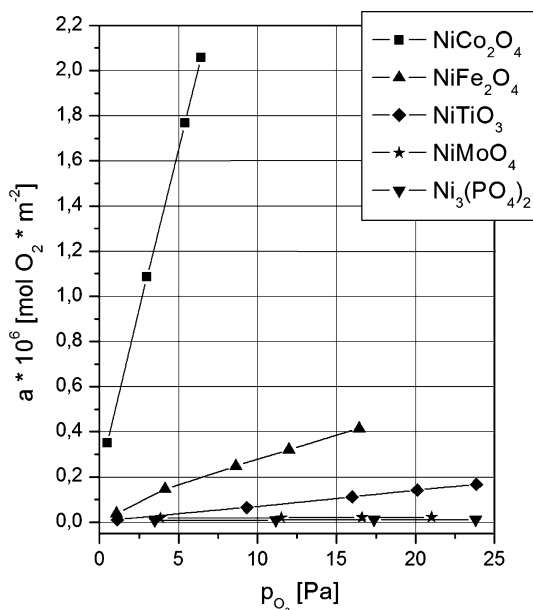
Calculated values of the ionic strengths of M–O (metal–oxygen) bonds in anionic group of oxysalts and binding energies for nickel Ni  $2p_{3/2}$  and oxygen O 1s (from XPS measurements) are shown in Table 2. The value of ionic strength of M–O bonds in oxysalts increases in the following order:  $\text{Ni}_3(\text{PO}_4)_2 < \text{NiMoO}_4 < \text{NiTiO}_3 < \text{NiFe}_2\text{O}_4 \approx \text{NiCo}_2\text{O}_4$ . The ionic strength of Co–O bond is slightly lower than of Fe–O, but this difference is negligible compared to the values for other samples. Therefore, the ionic strengths of M–O bonding in  $\text{NiFe}_2\text{O}_4$  and  $\text{NiCo}_2\text{O}_4$  are considered to be equal. As a consequence of an increase of ionic strength of M–O bonds in the anionic group of the oxysalt, the effective negative charge of oxygen ion should also increase. This phenomenon can be verified on the basis of XPS data. The values of binding energies of O 1s in examined oxysalts (Table 2) increase in the following order:  $\text{NiCo}_2\text{O}_4 < \text{NiFe}_2\text{O}_4 < \text{NiTiO}_3 < \text{NiMoO}_4 < \text{Ni}_3(\text{PO}_4)_2$ . The increase of bond strength between oxygen and metal atom indicates that electrons are much more involved in bonding and therefore, the negative charge of oxygen in anionic group of oxysalts decreases with an increase of binding energy. Taking into account the former conclusion, it is evident that the effective negative charge of oxygen ion in oxysalts increases as follows:  $\text{Ni}_3(\text{PO}_4)_2 < \text{NiMoO}_4 < \text{NiTiO}_3 < \text{NiFe}_2\text{O}_4 < \text{NiCo}_2\text{O}_4$ . According to Bagus et al. [12], the change in the O 1s binding energy between  $\text{NiCo}_2\text{O}_4$  and  $\text{Ni}_3(\text{PO}_4)_2$  corresponds to the change of the charge of oxygen ion equal approximately to 0.2.

$\text{NiCo}_2\text{O}_4$  has the lowest electron binding energy in nickel ion Ni  $2p_{3/2}$  (Table 2). It implicates the lowest ionization potential of nickel in  $\text{NiCo}_2\text{O}_4$  among all examined oxysalts. A low level of ionization potential in transition metals facilitates the oxidation of these metals. The highest ability of nickel in  $\text{NiCo}_2\text{O}_4$  to increase the oxidation state may explain the highest capacity of oxygen adsorption of  $\text{NiCo}_2\text{O}_4$  (Fig. 1). The binding energy of nickel in other oxysalts is higher than in  $\text{NiCo}_2\text{O}_4$  and increases as follows:  $\text{NiCo}_2\text{O}_4 < \text{NiFe}_2\text{O}_4 < \text{NiTiO}_3 < \text{NiMoO}_4 \approx \text{Ni}_3(\text{PO}_4)_2$ .

**Table 2** Values of ionic strength of M–O bonding in the anionic group of oxysalts and binding energies (BE) of Ni  $2p_{3/2}$  and O 1s in nickel oxysalts

Oxysalt	Ion $\text{M}^{n+}$	Ionic strength of M–O (%)	BE (core level) (eV)	
			Ni $2p_{3/2}$	O 1s
$\text{NiCo}_2\text{O}_4$	$\text{Co}^{3+}$	50.1	854.7	529.3
$\text{NiFe}_2\text{O}_4$	$\text{Fe}^{3+}$	51.2	855.2	530.0
$\text{NiTiO}_3$	$\text{Ti}^{4+}$	44.3	856.1	530.7
$\text{NiMoO}_4$	$\text{Mo}^{6+}$	28.9	856.5	530.8
$\text{Ni}_3(\text{PO}_4)_2$	$\text{P}^{5+}$	27.5	856.4	531.2

**Fig. 1** Oxygen adsorption isotherms at 653 K



### Oxygen chemisorption

The examined oxysalts exhibit different oxygen sorption capacities. The isotherms of oxygen adsorption at temperature 653 K for all samples are shown in Fig. 1. The number of moles of chemisorbed oxygen per unit area ( $1 \text{ m}^2$ ) of the sample surface, for constant equilibrium pressure and at particular temperature, increases in the following order:  $Ni_3(PO_4)_2 < NiMoO_4 < NiTiO_3 < NiFe_2O_4 < NiCo_2O_4$ . The smaller the ionization potential of the nickel ion, the higher the sorption of oxygen on the surface of oxysalt. As it was discussed elsewhere by Haber et al. [13, 14], these chemisorption relations might be explained by the analysis of the properties of isolated adsorption complexes on the basis of the ligand field theory. The observed relationship between the amount of chemisorbed oxygen and the type of anionic group in nickel oxysalts was also examined by Boreskov for cobalt oxysalts [14]. The references point that oxygen chemisorption depends strongly on the electro-donor properties of transition metal cation situated in the ligand field. These properties of nickel ions, which fluctuate with the varying strength of the ligand field, are responsible for the different oxygen sorption capacities of the examined oxysalts, but also affect their activity in propene oxidation process.

### Isopropyl alcohol conversion

Kinetic measurements of isopropyl alcohol conversion permit to determine acid–base and oxidation–reduction properties of the examined group of nickel oxysalts. The dehydration of isopropyl alcohol to propene is an indicator of acid–base properties of the catalysts [15, 16]. The activity of synthesized oxysalts in the dehydration to propene are compared in Fig. 2. As it is seen,  $NiMoO_4$  is the most

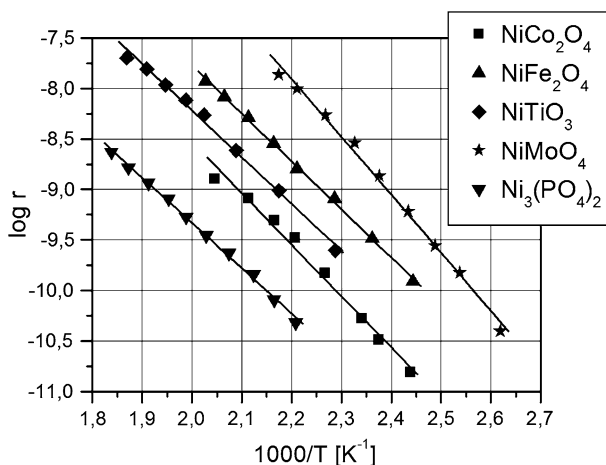


**Fig. 2** Arrhenius plots for the conversion of isopropyl alcohol to propene over nickel oxysalts

**Table 3** Selectivity and the total rate of catalytic conversion of isopropyl alcohol over nickel oxysalts

Catalyst	Selectivity (%)				Total rate (mol m <sup>-2</sup> s <sup>-1</sup> )	
	T = 445 K		T = 460 K		T = 445 K	T = 460 K
	Propene	Acetone	Propene	Acetone		
NiCo <sub>2</sub> O <sub>4</sub>	0.1	99.9	0.2	99.8	2.300 × 10 <sup>-7</sup>	3.496 × 10 <sup>-7</sup>
NiFe <sub>2</sub> O <sub>4</sub>	6.9	93.1	10.0	90.0	1.628 × 10 <sup>-8</sup>	2.510 × 10 <sup>-8</sup>
NiTiO <sub>3</sub>	8.2	91.8	11.2	88.8	5.127 × 10 <sup>-9</sup>	8.392 × 10 <sup>-9</sup>
NiMoO <sub>4</sub>	75.6	24.4	83.6	16.4	1.083 × 10 <sup>-8</sup>	2.748 × 10 <sup>-8</sup>
Ni <sub>3</sub> (PO <sub>4</sub> ) <sub>2</sub>	12.7	87.3	10.6	89.4	2.846 × 10 <sup>-10</sup>	7.261 × 10 <sup>-10</sup>

active catalyst in this reaction. Compared to other oxysalts, the selectivity to propene is also the highest (Table 3) for NiMoO<sub>4</sub>. This behavior may be due to the fact that, unlike other catalysts, the former possesses Brønsted type acid centers on the surface. As it is known, compounds containing transition metals with high oxidation state are able to create Brønsted type acid centers as a result of dissociative adsorption of water molecules [17]. Other catalysts reveal Lewis type acidity. Their activity in dehydration increases in the following order: Ni<sub>3</sub>(PO<sub>4</sub>)<sub>2</sub> < NiCo<sub>2</sub>O<sub>4</sub> < NiTiO<sub>3</sub> < NiFe<sub>2</sub>O<sub>4</sub>.

The influence of the oxide catalyst on the dehydrogenation of isopropyl alcohol to acetone can be used to determine the oxidation–reduction properties of this catalyst [18, 19]. Among all samples, NiCo<sub>2</sub>O<sub>4</sub> is the most active in dehydrogenation (Fig. 3). The activity decreases in the following order: NiFe<sub>2</sub>O<sub>4</sub>, NiTiO<sub>3</sub>, NiMoO<sub>4</sub>. The most passive is Ni<sub>3</sub>(PO<sub>4</sub>)<sub>2</sub>. All examined catalysts apart from NiMoO<sub>4</sub> reveal strong activity, mostly in the dehydrogenation reaction (Table 3). The low selectivity of NiMoO<sub>4</sub> in acetone formation is induced by very active Brønsted centers which favor the competitive parallel dehydration to propene.

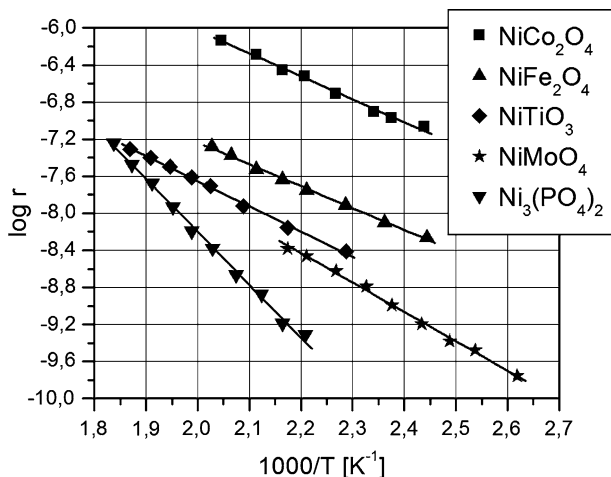


**Fig. 3** Arrhenius plots for conversion of isopropyl alcohol to acetone over nickel oxysalts

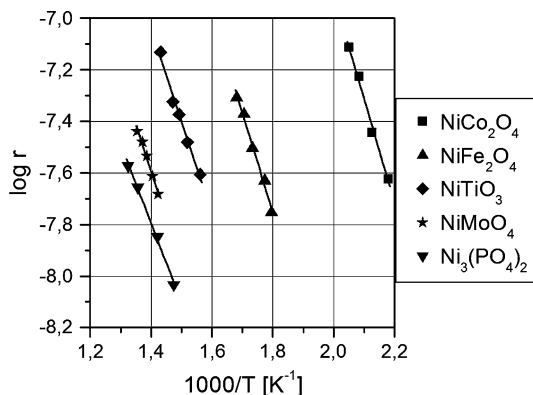
**Table 4** The values of activation energies of isopropyl alcohol conversion over nickel oxysalts

Catalyst	Activation energy (kJ/mol)	
	Dehydration to propene	Dehydrogenation to acetone
NiCo <sub>2</sub> O <sub>4</sub>	111.8	47.4
NiFe <sub>2</sub> O <sub>4</sub>	91.0	45.3
NiTiO <sub>3</sub>	91.3	52.1
NiMoO <sub>4</sub>	117.0	60.8
Ni <sub>3</sub> (PO <sub>4</sub> ) <sub>2</sub>	85.9	108.9

The values of total rate of conversion of isopropyl alcohol are collected in Table 3. The total activity of examined oxysalts increases in the following order: Ni<sub>3</sub>(PO<sub>4</sub>)<sub>2</sub> < NiTiO<sub>3</sub> < NiMoO<sub>4</sub> < NiFe<sub>2</sub>O<sub>4</sub> < NiCo<sub>2</sub>O<sub>4</sub>. This tendency repeats the pattern of catalyst behavior in the dehydrogenation to acetone, but with one exception. Catalyst NiMoO<sub>4</sub> is more active than NiTiO<sub>3</sub>. This is caused by the fact that NiMoO<sub>4</sub> reveals major activity in the dehydration of isopropyl alcohol to propene, whereas the other catalysts are most active in dehydrogenation to acetone.

The values of activation energies for both parallel reactions of isopropyl alcohol conversion are shown in Table 4. The activation energies of the dehydration process are comparable for all examined catalysts. In the dehydrogenation to acetone, the activation energies for all catalysts except Ni<sub>3</sub>(PO<sub>4</sub>)<sub>2</sub> are very low (45.3–60.8 kJ/mol). Much higher activation energy (108 kJ/mol) in the dehydrogenation for nickel phosphate is probably caused by the number of oxidation–reduction active centers. Contrary to other catalysts with two different transition metals centers, Ni<sub>3</sub>(PO<sub>4</sub>)<sub>2</sub> has only one active center for dehydrogenation (Ni<sup>2+</sup>), which causes higher activation energy.



**Fig. 4** Arrhenius plots for propene oxidation over nickel oxysalts**Table 5** The values of activation energies, temperatures at a given rate and selectivity of propene oxidation over nickel oxysalts

Catalyst	Activation energy (kJ mol <sup>-1</sup> )	Temperature (K) ( <sup>a</sup> $r = 25.1 \times 10^{-9}$ mol m <sup>-2</sup> s <sup>-1</sup> )	Selectivity (%) (at reaction rate $r = 25.1 \times 10^{-9}$ mol m <sup>-2</sup> s <sup>-1</sup> )			
			Acrolein	Acetaldehyde	Ethyl acetate	Total oxidation
NiCo <sub>2</sub> O <sub>4</sub>	77.3	461	6.6	3.2	–	90.2
NiFe <sub>2</sub> O <sub>4</sub>	73.9	568	37.3	8.4	2.3	52.0
NiTiO <sub>3</sub>	68.9	643	42.4	14.8	3.4	39.4
NiMoO <sub>4</sub>	69.6	714	55.5	19.1	4.2	11.2
Ni <sub>3</sub> (PO <sub>4</sub> ) <sub>2</sub>	58.7	748	71.8	5.4	1.2	21.6

<sup>a</sup> Rate of the reaction at the given temperature

### Propene oxidation

The activity of examined catalysts in propene oxidation is presented in Fig. 4. The values of activation energy of propene oxidation, reaction temperatures at which the reaction rate is equal to  $25.1 \times 10^{-9}$  mol m<sup>-2</sup> s<sup>-1</sup> and values of the selectivity of oxidation at a given reaction rate, for all oxysalts are presented in Table 5. The reaction selectivity, either for catalytic or for noncatalytic processes, depends strongly on temperature. Therefore, in practice, for comparing the selectivity of different catalysts in the reaction, it is important to carry out experiments in the same range of temperature. Unfortunately, the activity of the examined oxysalts in propene oxidation differs significantly, so it was impossible to preserve the same temperature conditions during catalytic tests. For comparing the selectivity values of all samples, it was necessary to calculate selectivity of each oxysalt at one value of reaction rate i.e. at the same reaction yield.

NiCo<sub>2</sub>O<sub>4</sub> reveals the highest activity in propene oxidation (Fig. 4). This catalyst also shows the highest selectivity in the total oxidation of propene (Table 5). The total oxidation of olefins proceeds when electrophilic forms of oxygen (O<sub>2</sub><sup>-</sup> and O<sup>-</sup> ions) are present on the surface of the catalyst [8]. NiCo<sub>2</sub>O<sub>4</sub> has strong oxidation–reduction

properties and high capacity of oxygen adsorption, which enable effective generation of electrophilic forms of oxygen on the catalyst surface. It explains the high activity of  $\text{NiCo}_2\text{O}_4$  in the total oxidation of propene. The catalyst  $\text{NiFe}_2\text{O}_4$  has lower capacity of oxygen adsorption and weaker oxidation–reduction properties than  $\text{NiCo}_2\text{O}_4$ . As a consequence,  $\text{NiFe}_2\text{O}_4$  is less active in propene oxidation (Fig. 4). However,  $\text{NiFe}_2\text{O}_4$  is more selective in acrolein formation (nondestructive oxidation) (Table 5). This tendency remains the same for other examined oxysalts. The lower the capacity of oxygen adsorption and the weaker the oxidation–reduction properties, the lower the activity in propene oxidation and the higher the selectivity in acrolein formation.

Generally, the selectivity of oxysalts in total oxidation drops with the decrease of the capacity of oxygen adsorption and oxidation–reduction properties. All samples except  $\text{NiMoO}_4$  exhibit similar behavior (Table 5). The selectivity of total oxidation over  $\text{NiMoO}_4$  is almost half the value over  $\text{Ni}_3(\text{PO}_4)_2$ , despite the better capacity of oxygen adsorption and stronger oxidation–reduction properties of  $\text{NiMoO}_4$ . This different behavior could be explained by the fact that, unlike other oxysalts,  $\text{NiMoO}_4$  reveals strong acid–base properties associated with Brønsted type acidity (see “[Isopropyl alcohol conversion](#)” section). The oxidation of organic species over catalysts of this type involves the generation of the nucleophilic form of oxygen (lattice ions  $\text{O}^{2-}$ ), and leads to nondestructive oxidation products. The formation of significant amounts of acetaldehyde, which is a product of propene oxidation involving the rupture of double bond of the olefin, is possible due to the acid properties of  $\text{NiMoO}_4$ . The mechanism of this reaction involves the activation of the double bond by the nucleophilic attack of oxygen. This activation is possible only by the adsorption of the propene molecule by the electron-rich double bond on the strong acid active center. It causes creation of carbocation and, as a result, sensitizes double bond to nucleophilic attack of  $\text{O}^{2-}$  ion.

Oxysalts with high capacity of oxygen adsorption and high activity in propene oxidation show high activation energy values and high contribution in destructive oxidation (with C–C bond cleavage). The lower oxygen sorption capacity of oxysalts causes a decrease of their activity but on the other hand entails a decrease of activation energy of propene oxidation.

## Conclusions

The capacity of oxygen adsorption of the examined oxysalts, which depends on the electrodonor properties of nickel ion, can be correlated with activity and selectivity of propene oxidation over these catalysts. On the basis of the presented results, we can conclude that oxysalts with high oxygen adsorption capacity containing a transition metal ion with strong electrodonor properties are active in total oxidation process (electrophilic oxidation). The lower the ionization potential of the transition metal ion and greater participation of ion bonding in anion group of the oxysalt, the higher the activity of the catalyst in the total oxidation of hydrocarbons. In contrast, oxysalts with moderate oxygen adsorption capacity, containing metal ions with weaker electrodonor properties, are most active in the selective oxidation (nucleophilic oxidation) of hydrocarbons.

## References

1. Viswanadham N, Shido T, Iwasawa Y (2001) Performances of rhenium oxide-encapsulated ZSM-5 catalysts in propene selective oxidation/ammoxidation. *Appl Catal A Gen* 219:223–233
2. Campbell CT (1985) Cesium-promoted silver(111): model studies of selective ethylene oxidation catalysts. *J Phys Chem* 89:5789–5795
3. Serefin JG, Liu AC, Seyedmonir SR (1998) Surface science and the silver-catalyzed epoxidation of ethylene: an industrial perspective. *J Mol Catal A* 131:157–168
4. Centi G, Perathoner S (2001) Reaction mechanism and control of selectivity in catalysis by oxides: some challenges and open questions. *Int J Mol Sci* 2:183–196
5. Duc DT, Ha HN, Fehrman R, Riisager A, Le MT (2011) Selective oxidation of propylene to acrolein by silica-supported bismuth molybdate catalysts. *Res Chem Intermed* 37:605–616
6. Bielański A, Haber J (1991) Oxygen in catalysis. Marcel Dekker Inc, New York
7. Libre JM, Barbaux Y, Grzybowska B, Bonnelle JP (1982) A surface potential study of adsorbed oxygen species on a  $\text{Bi}_2\text{Mo}_3\text{O}_{12}$  catalyst. *React Kinet Catal Lett* 20:249–254
8. Haber J (1997) In: Grasselli RK, Oyama ST, Gaffney AM, Lyon JE (eds) *Studies in surface science and catalysis*. Elsevier, Amsterdam
9. Bielański A, Haber J (1979) Oxygen in catalysis on transition metal oxides. *Catal Rev* 19:1–41
10. Haber J, Turek W (2000) Kinetic studies as a method to differentiate between oxygen species involved in the oxidation of propene. *J Catal* 190:320–326
11. Anthony MT (1983) In: Brigs D, Seah MP (eds) *Practical surface analysis by Auger and X-ray photoelectron spectroscopy*. Wiley, London
12. Bagus PS, Bauschlicher ChW (1980) Core binding-energy shifts for free negative ions of oxygen:  $\text{O}^0$  to  $\text{O}^{2-}$ . *J Electron Spectrosc Relat Phenom* 20:183–190
13. Haber J, Mielczarska E (1979) Wlijanje elektronných swoistw słoznych okisnych sistem na adsorpcju kisloroda. *Zurn Fiz Chim* 53:2909–2914
14. Dziewięcki Z, Haber J (1975) Chemisorption of oxygen on cobalt oxysalts of different bond ionicity. *React Kinet Catal Lett* 3:55–62
15. Turek W, Haber J, Krowiak A (2005) Dehydration of isopropyl alcohol used as an indicator of the type and strength of catalyst acid centers. *Appl Surf Sci* 252:823–827
16. Turek W, Lapkowski M, Debiec J, Krowiak A (2005) Studies of the activity of catalysts based on heteropolyacids. *Appl Surf Sci* 252:847–852
17. Busca G (1999) The surface acidity of solid oxides and its characterization by IR spectroscopic methods. An attempt at systematization. *Phys Chem Chem Phys* 1:723–736
18. Turek W, Lapkowski M, Krowiak A, Teterycz H, Klimkiewicz R (2007) Evaluation of semiconducting sensor materials on the basis of catalytic test reaction. *Appl Surf Sci* 253:5920–5924
19. Strzeżik J, Krowiak A, Turek W, Kozieł K, Szperlich P (2009) Morphology and conductivity of polymeric support as the key factors modifying catalytic activity of Keggin type heteropolyacids dispersed in poly(*N*-methylpyrrole) and polypyrrole matrices. *Catal Lett* 127:226–231